Dielectric Spectrum Extraction of Liquids Using Noncontact Microwave Split Ring Resonator

Wendi Zhu, *Graduate Student Member, IEEE*, Masoud Baghelani, *Senior Member, IEEE*, and Ashwin K. Iyer, *Senior Member, IEEE*

***Abstract*— This article presents a novel method for broadband dielectric spectroscopy of liquids utilizing a noncontact microwave split ring resonator (SRR). The proposed approach leverages the multiharmonic property of the microwave resonator to extract the permittivity of the liquid-under-test (LUT) at resonance frequencies. By fitting these extracted values using the Debye model, both the real and imaginary dielectric spectra of the LUT can be determined across a wide frequency range. The proposed method requires a one-time calibration process to ensure high accuracy. An experiment employing five calibration samples and five test samples was performed to validate the effectiveness of the proposed method. The results of the extracted permittivity spectrum using the proposed method are compared with those from a commercial dielectric probe. The proposed method exhibits high accuracy with a root mean square error of 0.59 for ϵ' values at the resonance frequencies. For the extracted Debye model parameters, the proposed method achieves reasonable precision with percentage errors of 1.40% for ϵ_s, 12.68% for ϵ_∞, and 7.86% for τ and is a cost-effective and accurate solution for dielectric spectroscopy. Due to its planar structure, the microwave SRR can be seamlessly integrated into various systems, holding potential for applying this method in microwave sensing, noninvasive biological sensing, oil and gas industries, and other fields requiring dielectric spectroscopy.**

***Index Terms*— Debye model, dielectric spectroscopy, microwave sensors, noncontact measurement, split ring resonator (SRR).**

I. Introduction

DIELECTRIC spectroscopy is an essential technique for investigating the dielectric properties of materials, playing a crucial role in diverse applications such as biosensing, real-time analysis of chemical reactions, oil and gas industries, power engineering, contamination analysis, and much more. Many methods have been suggested by scientists and utilized by industries for dielectric spectroscopy, covering various frequency ranges from low frequencies to microwaves and optical frequencies [1], [2], [3].

The transmission and reflection line method has been extensively studied in [4], [5], [6], and [7]. This method usually involves direct contact with the sample and typically requires the sample to be in a specific form, such as a slab with a constant thickness [5]. Consequently, this method suffers from limitations in being unable to perform noninvasive and nondestructive testing. Due to its capability of performing semi-invasive spectroscopy, the open-ended coaxial cable probe method achieved a great deal of interest in industries with many commercialized products available in the market [8], [9], [10], [11]. However, the accuracy of this method is limited by the potential presence of air gaps. It also exhibits limited accuracy at lower frequencies, especially below 200 MHz, and tends to be less precise for materials with low dielectric constants and loss factors [12]. Free-space dielectric spectroscopy techniques offer great opportunities for measuring the dielectric properties of materials in diverse environments [13], [14], [15]. Using this method, noninvasive high-frequency spectroscopy is possible but at the cost of requiring a large and flat material under test (MUT) as well as extreme sensitivity to the placement of the transmitting and receiving antennas and the MUT. On the other hand, resonant methods can achieve high accuracy with the capability of performing dielectric spectroscopy over a small volume of MUT [16], [17], [18], [19], [20], [21]. The utilization of microfluidic channels with the resonant method has achieved an ultrahigh sensitivity requiring only a microliter volume of samples. This approach has found applications across diverse fields, including the detection of glucose, equol, or other compounds in energy and biomedical applications [23], [24], [25].

Planar microwave sensors have been utilized widely in the past decades for sensing applications. Due to their moderate quality factor, decent sensitivity, and ability to perform noncontact sensing at extremely low cost, many biomedical and industrial sensors have been developed based on this technology [26], [27]. When an MUT is introduced to the sensor, the sensing principle of planar microwave sensors can be based on its variations in resonant frequency [28], [29], Q factor [30], amplitude [31], or phase [32], [33]. There are many types of planar microwave sensors, including frequency shift sensors, Q-based resonant sensors, phase variation sensors, and differential sensors, each leveraging one or more of the aforementioned sensing principles [28], [29], [30], [31], [32], [33]. Frequency shift sensors are usually implemented with resonators and are one of the most common types [19], [20]. The sensing information can be extracted based on the variation of their resonance frequency in response to changes in their surrounding environment. Another valuable property

Manuscript received 24 February 2024; revised 29 March 2024; accepted 31 March 2024. This work was supported in part by the Innovation for Defense Excellence and Security (IDEaS) Program from the Department of National Defense (DND). *(Corresponding author: Wendi Zhu.)*

The authors are with the Department of Electrical and Computer Engineering, University of Alberta, Edmonton, AB T6G 1H9, Canada (e-mail: wzhu7@ualberta.ca; baghelan@ualberta.ca; iyer@ece.ualberta.ca).

Color versions of one or more figures in this article are available at https://doi.org/10.1109/TMTT.2024.3386109.

Digital Object Identifier 10.1109/TMTT.2024.3386109

of resonators is their capability for Q-based measurements, allowing the extraction of sensing information based on the Q-factor of the sensor [34]. Phase variation sensors, often implemented with a long and typically meandered transmission line, allow the sensing information to be extracted through the phase measurements at a single frequency [35]. Differential sensors usually consist of two sensing elements, which typically have a symmetrical layout and can be independent or coupled to each other [36], [37], [38]. One main advantage of differential sensors is the mitigated impact of environmental factors, such as temperature, as these factors do not disrupt the inherent symmetry of the sensor design [39], [40]. Various techniques are utilized to improve the performance of planar microwave sensors, such as employing active feedback circuitry to offset losses for enhancing quality factors and improving the sensor resolution [41]. Innovations like chipless RFID tags have been developed to enable wireless sensing [42], [43]. Machine learning techniques have been utilized for temperature compensation [44], [45]. Moreover, multiresonance structures have been explored to enhance selectivity and enable multivariable analysis [46].

While numerous studies have proposed the use of microwave planar resonators for extracting permittivity values at a single frequency [47], [48], [49], a method for determining the dielectric spectrum for both the real and imaginary parts covering a wide frequency band remains missing. In this work, we propose a method to perform wideband dielectric spectroscopy using a traditional planar microwave split ring resonator (SRR). Multiple harmonics of the microwave SRR are utilized for sampling the dielectric spectrum of the MUT. By analyzing the frequency shifts of the resonator's harmonics, it is possible to extract the permittivity of the target MUT at the resonance frequencies. According to the Debye model, the dielectric spectrum of most materials in the microwave frequency range is changing smoothly. Consequently, by using a few sample points, we can reconstruct the entire dielectric spectrum of the target MUT using the Debye model. A one-time experimental calibration with known materials is required in this method to enhance the precision of the measurements. After calibration, the permittivity spectrum of various MUTs may be extracted with reasonable accuracy. The proposed method in this work offers a low-cost, noninvasive, wideband dielectric spectroscopy solution that can be employed in various applications such as chemical analysis, oil and gas industries, and biosensing.

The rest of this article is structured as follows. Section II outlines the proposed method for conducting wideband dielectric spectroscopy using microwave SRRs. Section III offers a comprehensive validation of the proposed method and provides a detailed discussion of the experimental results, followed by a conclusion in Section IV.

II. Dielectric Spectroscopy Using Microwave SRR

This work utilized the multiharmonic mechanism of a microwave SRR for sampling the dielectric permittivity of the MUTs at various frequencies to extract their dielectric spectra. A simple microwave SRR is developed with microstrip technology as shown in Fig. 1(a), which presents multiple

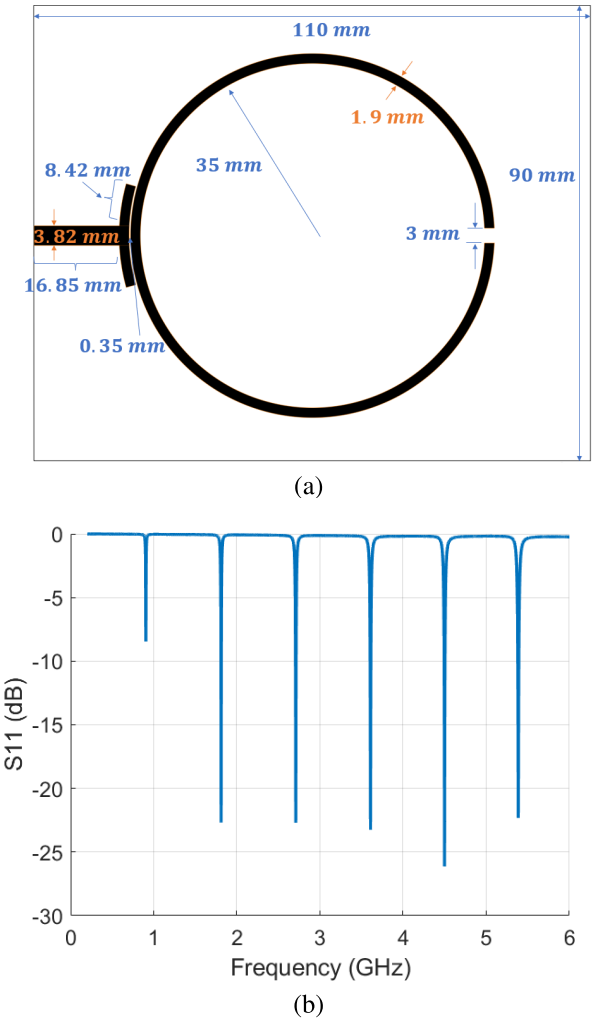

Fig. 1. (a) Dimensions of the microwave SRR utilized in this work. (b) $S11$ response from HFSS simulation, which shows a multiharmonic response with decent quality factor.

resonance frequencies as shown in the simulation result in Fig. 1(b). The SRR is designed on a Rogers RO3003 substrate ($\epsilon_r = 3$) with a substrate thickness of 1.52 mm. The resonator has a radius of 35 mm and a splitting gap of 3 mm, where the 3-mm splitting gap forms a sensitive region suitable for placing the MUT for sensing applications. The resonator is excited through a 50 Ω transmission line with a width of 3.82 mm that is capacitively coupled to the SRR with a coupling gap of 0.35 mm. This coupling allows for the transfer of energy from the transmission line to the SRR, exciting its resonant modes, resulting in notches in the return loss response. At resonances, the incident energy is effectively transferred and retained by the resonator and eventually dissipated as ohmic loss, dielectric loss, and radiation [53]. To investigate power dissipation at the resonances, we conducted an HFSS simulation on the bare sensor, which shows that the majority of the incident power is dissipated as ohmic and dielectric losses, with a smaller portion dissipated as radiation loss. For instance, at the first resonance, 72.67% of the incident power is dissipated as ohmic and dielectric losses, 11.74% as radiation, and 15.59% is reflected.

The resonance frequencies of a microwave SRR can be calculated as follows [53]:

$$f_{r,n} = \frac{nc}{l_{\text{eff}}\sqrt{\epsilon_{\text{eff}|f_{r,n}}}} \tag{1}$$

where n is the harmonic number, c is the speed of light in the free space, $f_{r,n}$ is the nth resonance frequency of the resonator, l_{eff} is the effective length of the resonator, and $\epsilon_{\text{eff}|f_{r,n}}$ is the effective permittivity due to the ambient dielectric environment, including the substrate, of the sensor at the nth resonance frequency. The introduction of a new MUT to the resonator leads to a change in ϵ_{eff}, resulting in different resonance frequencies. The shifts in the nth resonance frequency can be calculated as follows:

$$\Delta f_{r,n} = f_{r,n|\text{air}} - \frac{nc}{l_{\text{eff}}\sqrt{\left(\epsilon_{\text{eff}|f_{r,n}}\right)_{\text{MUT}}}} \tag{2}$$

where $f_{r,n|\text{air}}$ is the nth resonance frequency of the structure with air as the MUT. The change in resonance frequency, denoted as $\Delta f_{r,n}$, serves as an indicator of how the dielectric properties of the MUT impact the sensor's response. With $f_{r,n|\text{air}}$ available from measurements, $\Delta f_{r,n}$ can be calculated as a function of the effective permittivity in the presence of the MUT. Therefore, by measuring $\Delta f_{r,n}$, it is possible to determine the permittivity of the MUT at the resonance frequencies.

A. Debye Relaxation Model for Dielectric Materials

Before delving into the details of the proposed method for dielectric spectroscopy, it is essential to provide an overview of the Debye relaxation model for dielectric materials [50], [51]

$$\epsilon(f) = \epsilon_\infty + \frac{\epsilon_s - \epsilon_\infty}{1 + (i2\pi f\tau)} \tag{3}$$

where $\epsilon(f)$ is the complex dielectric permittivity as a function of frequency, ϵ_∞ is the permittivity at the high-frequency limit, ϵ_s is the permittivity at static or low frequency, and τ is the characteristic relaxation time constant. From (3), the real and imaginary parts of the dielectric permittivity can be calculated as follows:

$$\epsilon' = \epsilon_\infty + \frac{\epsilon_s - \epsilon_\infty}{1 + (2\pi f\tau)^2} \tag{4}$$

$$\epsilon'' = \frac{(\epsilon_s - \epsilon_\infty)2\pi f\tau}{1 + (2\pi f\tau)^2}. \tag{5}$$

Since there are three unknown parameters (ϵ_s, ϵ_∞, and τ) in (3), a minimum of three independent equations is necessary to uniquely determine these parameters when analyzing a material. Consequently, at least three harmonics and their corresponding frequency shifts from the resonator are required to reconstruct the dielectric spectrum of the MUT based on the Debye model. As the proposed method utilizes more than three harmonics, the Debye model parameters can be determined through a curve-fitting process, leveraging the abundance of data points to minimize the impact of noise.

In this study, a frequency band of interest ranging from 0.5 to 6 GHz is chosen to demonstrate the proof of concept

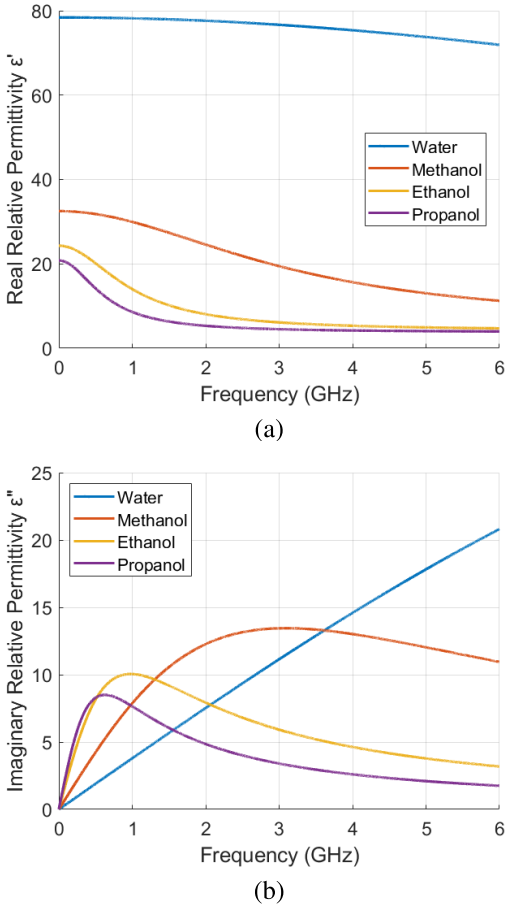

Fig. 2. (a) Real and (b) imaginary parts of dielectric permittivity of various liquids over the frequency of interest, which exhibits a smooth variation, allowing the permittivity spectrum to be reconstructed using only a few sampling points.

for our proposed dielectric spectrum extraction method. This decision is guided by two key considerations. First, we need a frequency band for the dielectric permittivity of the MUTs to change over, and the chosen frequency band of interest provides sufficient bandwidth to exhibit large variations in the dielectric permittivity of the MUTs. Second, we utilized the Copper Mountain R60 1-Port vector network analyzer (VNA) to measure the frequency response of our SRR sensor, which can read frequencies up to 6 GHz, aligning with the chosen frequency band of interest.

It is informative to revisit the Debye model for various materials in the frequency band of interest. As an example, the Debye models for water, methanol, ethanol, and propanol are illustrated in Fig. 2. Table I presents the Debye model parameters for these samples reported in [52]. As shown in Fig. 2, these samples exhibit a smooth variation in their permittivity spectra, enabling the reconstruction of the entire permittivity spectrum using only a few sample points.

B. Proposed Method for Dielectric Spectroscopy

Fig. 3 presents the flowchart of the proposed method for dielectric spectroscopy. The process starts with designing a multiharmonic microwave SRR with a proper fundamental resonance frequency. Since the frequency band of interest

TABLE I
DEBYE MODEL PARAMETERS FOR VARIOUS LIQUIDS AT 20 °C [52]

Material	ϵ_s	ϵ_∞	$\tau(ps)$
Water	80.4	5.2	9.4
Methanol	33.6	5.7	53.1
Ethanol	25.1	4.3	143.3
Propanol	19.0	3.2	291.9

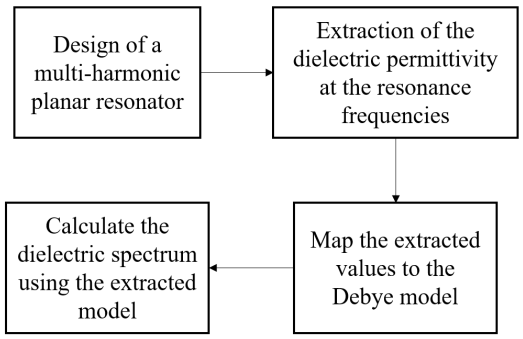

Fig. 3. Flowchart of the proposed method for dielectric spectroscopy.

in this work is between 0.5 and 6 GHz, a fundamental resonance frequency that is slightly below 1 GHz would be appropriate to provide six harmonics within this frequency range. The second step focuses on the extraction of the dielectric permittivity at the resonance frequencies, which is a crucial step in defining the accuracy of the method. Due to the complex geometry of the measurement setups, it is very challenging to determine the dielectric permittivity of the MUT from the frequency shifts analytically. However, using some calibration materials with commercial dielectric spectroscopy equipment, it is possible to calibrate the setup for determining the dielectric permittivity values experimentally. Section III-C provides the details of this calibration process. The third step in the proposed method involves mapping the extracted dielectric permittivity values at the resonance frequencies to the Debye model based on (4).

In this work, we choose to extract the real part of the permittivity instead of the imaginary part to fit the Debye model. This decision is based on the straightforward nature of the real part extraction, as the shift in the resonance frequency of a passive resonator primarily depends on the real part of the dielectric permittivity [22], [53]. To illustrate this, we performed an HFSS simulation where an ideal cylindrical MUT was placed on top of our SRR, with the MUT ϵ_r varying from 1 to 50 and the loss tangent varying from 0 to 1. The resulting fundamental resonance frequency of our SRR is provided in Fig. 4.

Fig. 4 shows that changes in ϵ_r significantly impact the resonance frequency of our SRR, yielding a 26.84% shift as MUT ϵ_r changes from 1 to 50. In contrast, changes in the loss tangent do not have much impact on the resonance frequency, producing a maximum of 2.4% shift as tanδ changes from 0 to 1 with MUT $\epsilon_r = 50$. Therefore, the resonance frequency shift of our SRR is predominantly determined by the real part of the permittivity, with the effect of the imaginary part considered negligible in comparison. An alternative method

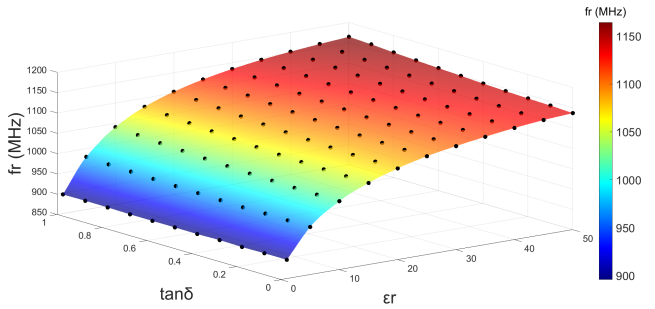

Fig. 4. Fundamental resonance frequency f_r of our SRR versus different MUT permittivity ϵ_r and loss tangent tanδ, which shows that f_r primarily depends on ϵ_r, with the effect of tanδ considered negligible in comparison.

involves extracting the imaginary part of the permittivity using the Q-factor. It is important to note, however, that the Q-factor is dependent on both the real and imaginary parts of the dielectric permittivity [21]. Therefore, the choice for real part extraction is considered more straightforward as the resonance frequency shift of our SRR mainly depends on the real part of the permittivity, with the impact of the imaginary part considered negligible in comparison.

After establishing the Debye model parameters through a fitting process applied to the extracted data, the real and imaginary parts of the dielectric permittivity spectrum can be calculated using (4) and (5). Using this method, it becomes possible to calculate the complex dielectric permittivity of the MUT across a wide frequency range that extends beyond the measured frequency. The Section III covers the practical aspects of the proposed method, providing a detailed discussion of experimental results.

III. EXPERIMENTS AND DISCUSSIONS

This section provides the experimental results and discusses the required steps to compute the dielectric spectrum of liquids using the proposed method. The experiment utilized ten samples, which were classified into two separate groups: a "calibration" group and a "test" group, each consisting of five samples. The descriptions of these samples are provided in Table II. The calibration liquids were chosen to provide a sufficiently wide range of permittivity values, spanning from the higher limit represented by water to the lower limit represented by propanol. The remaining three calibration liquids were selected randomly to cover permittivity values between these limits. The selection of calibration liquids ensures that the permittivity of the test liquids falls within the permittivity range covered by the calibration liquids.

Fig. 5 outlines the experiment steps in this study. The experiment begins with extracting the dielectric spectrum of calibration liquids using a commercial dielectric probe shown in Fig. 6: an open mode probe method dielectric constant and dielectric loss tangent measurement system, DPS16, from KEYCOM Characteristic Technologies through a ZVA 67 VNA from Rohde&Schwarz© from 0.5 to 6 GHz. By introducing the calibration liquids to the resonator and analyzing the resonance frequency shifts, the calibration equations can be extracted to describe the relationship between ϵ_r' and $\Delta f_{r,n}$ at the resonance frequencies. After the calibration

TABLE II
SAMPLES FOR THE EXPERIMENT

Sample	Description	Group
Water	Pure water	Calibration
PR	Pure Propanol	Calibration
EG	Ethylene Glycol	Calibration
ET	Pure Ethanol	Test
M1P9	10% Methanol + 90% Propanol	Calibration
M2P8	20% Methanol + 80% Propanol	Test
M3P7	30% Methanol + 70% Propanol	Test
M4P6	40% Methanol + 60% Propanol	Calibration
M2E1P7	20% Methanol + 10% Ethanol + 70% Propanol	Test
M3E1P6	30% Methanol + 10% Ethanol + 60% Propanol	Test

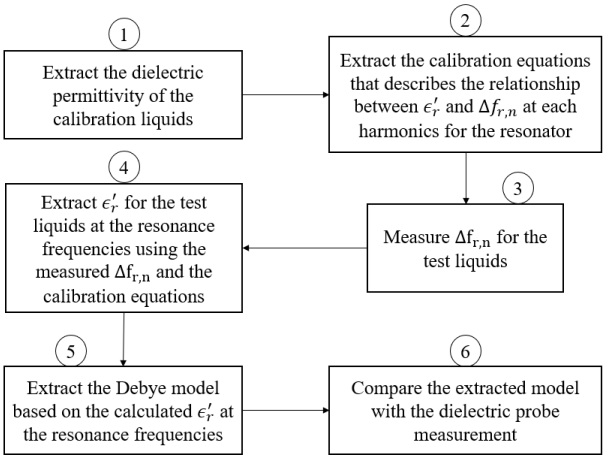

Fig. 5. Experiment steps for dielectric spectroscopy using the proposed method.

phase, we proceed to measure the resonance frequency shifts $\Delta f_{r,n}$ for the test liquids. This allows us to extract the ϵ_r' at the resonance frequencies using the calibration equations. Subsequently, by performing curve fitting on the extracted values, the Debye model parameters for the test liquids can be determined, which allows us to calculate the entire dielectric spectrum covering up to the frequency beyond our measurement range. To validate the accuracy of the proposed method, the extracted Debye model parameters are compared with the measurements from the commercial dielectric probe. Detailed information on the experimental setup and a comprehensive description of the experiment using the proposed method for dielectric spectroscopy are provided in the following sections.

A. Experimental Setup

The utilized sensor in this work is a simple microwave SRR with a ring radius of 35 mm and a splitting gap of 3 mm, illustrated in Fig. 1(a). The sensor is fabricated on an RO3003 substrate from Rogers Corporation with $\epsilon_r = 3$, $\tan\delta = 0.0013$, substrate thickness of 1.52 mm, and a copper metalization thickness of 35 μm. A low-loss polymer container with a bottom diameter of 47 mm and a wall thickness of 0.45 mm is placed on top of the sensor to hold the liquids for measurements. The liquid container is placed to cover the splitting gap of the SRR, an area known for its high sensitivity. Since the liquid container is quite large, precise centering onto the splitting gap is unnecessary. Full coverage of the

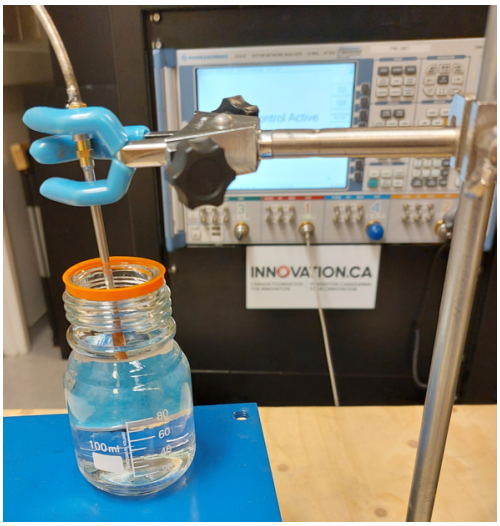

Fig. 6. Extracting dielectric spectrum of the calibration liquids using a commercial dielectric probe: an open mode probe method dielectric constant and dielectric loss tangent measurement system, DPS16, from KEYCOM Characteristic Technologies through a ZVA 67 VNA from Rohde&Schwarz©from 0.5 to 6 GHz.

resonator including the coupling gap is avoided since it may increase the unwanted sensitivity of the response of the sensor to small movements or dislocation of the container over the sensor for each measurement. The material of the container does not affect the results of the experiments while being low loss. However, the wall thickness of the container can impact the sensitivity of the system [54], [55]. A thicker wall would position the liquid-under-test (LUT) farther from the sensor, resulting in a reduced frequency shift in the sensor's resonance frequency for a specific dielectric permittivity variation in the LUT. Therefore, a relatively thin container is selected for this work to maintain the sensitivity of the proposed dielectric spectroscopy system. To prevent unwanted movement of the container, a 3-D printed polylactic acid (PLA) holder structure is employed to fix the location of the container. The effect of the alignment between the sensor and the liquid container, along with other setup factors, can be effectively addressed through a calibration process outlined in Section III-C.

Fig. 7 presents the experimental setup and the measured reflection response of the fabricated sensor loaded with an empty container. In the frequency range of interest from 0.5 to 6 GHz, the sensor presents resonance frequencies at 0.873, 1.734, 2.596, 3.464, 4.328, and 5.217 GHz. The measurements are performed using a Copper Mountain R60 1-Port 6 GHz VNA with a frequency range from 1 MHz to 6 GHz. A total of 100 000 measurement points are employed with an IFBW of 30 kHz. These configurations ensure a frequency interval of approximately 60 kHz between each pair of adjacent measurements, capturing sufficient frequency variation for subsequent data analysis.

B. Stability Analysis for the Experimental Setup

The experiment was conducted in a controlled laboratory environment with a constant temperature of 20 °C. To assess the stability of the experimental setup, a time-based mea-

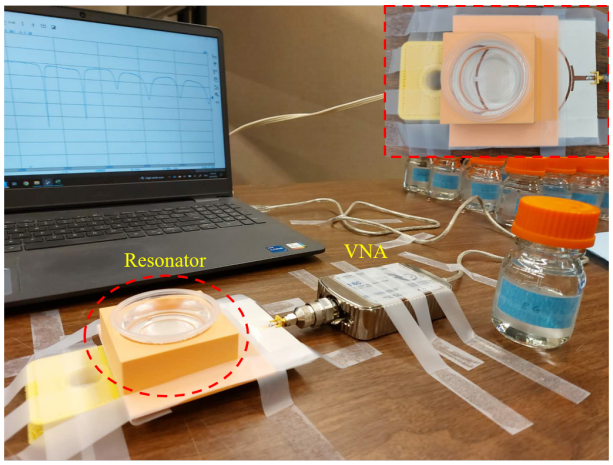

(a)

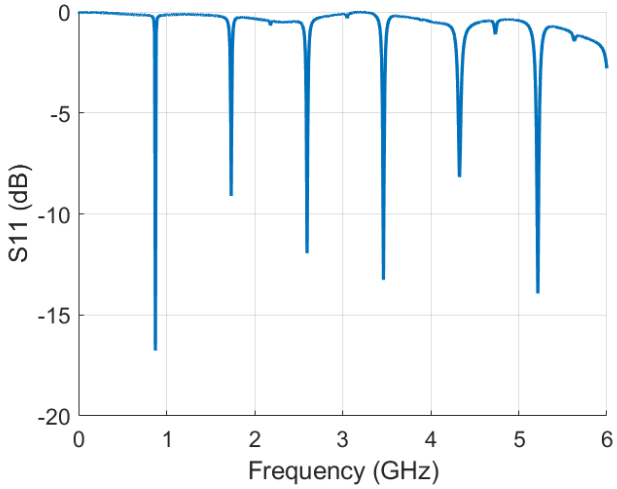

(b)

Fig. 7. (a) Experimental setup including the zoomed version of the microwave SRR. (b) Reflection response of the sensor loaded with the empty container.

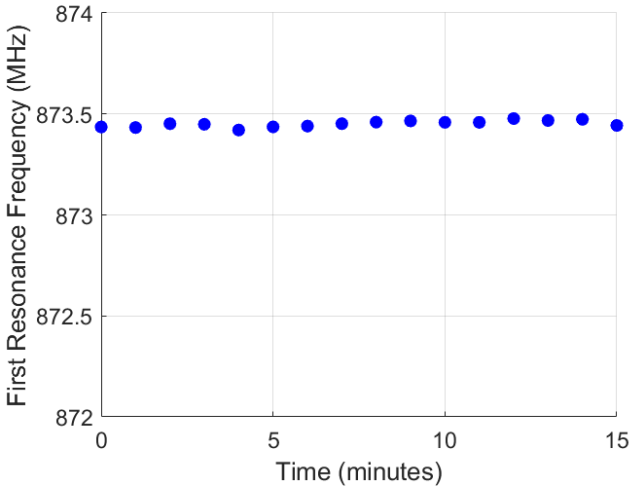

Fig. 8. First resonance frequency of the sensor versus time when loaded with an empty container, which shows almost no variation over time.

surement was conducted using a custom LabVIEW interface to monitor the first resonance frequency of the sensor when loaded with an empty container. As illustrated in Fig. 8, it is evident that the sensing system exhibits almost no variation over time, confirming the stability of the experimental setup.

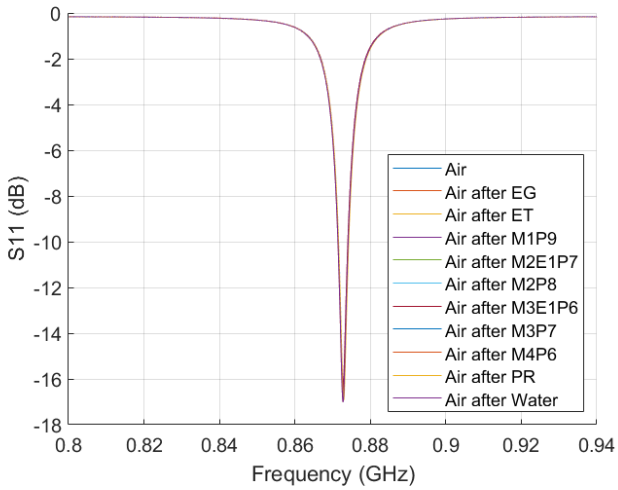

Fig. 9. $S11$ response of the sensor around the first resonance when unloaded after each liquid, showing high repeatability of the measurement.

To investigate the repeatability of the measurements, the $S11$ responses of the sensor around the first resonance are measured after unloading each of the liquids used in this experiment. As shown in Fig. 9, the $S11$ measurements exhibit a high level of repeatability for the sensor unloaded after each liquid.

Another common concern that frequently arises with liquid testing is the potential for inaccurate volume measurement of the LUT. This issue can severely impact the experiment results since the microwave sensor is highly sensitive to environmental changes, encompassing both variations in the volume and dielectric permittivity of the LUT. To overcome this challenge, a robust mechanism is developed in this work to mitigate the need for a highly precise volume measurement. Since the impact of dielectric permittivity variation in the sensor's ambient environment decreases with increasing distance from the resonator, it can be predicted that beyond a certain volume threshold, any additional volume would have a negligible effect on the resonance frequencies. Consequently, small volume variations beyond that point would not introduce detectable errors in the measurement, making the experiment volume-insensitive. To address this practical concept, the first resonance frequency of the resonator loaded with various volumes of ethanol is measured, and the results are presented in Fig. 10. It can be seen that the first resonance frequency of the sensor remains relatively constant when the volume of ethanol exceeds 30 mL. In the subsequent experiments, a volume of 45 mL is chosen for the LUT, which is well beyond the threshold determined in this experiment. This choice improves the overall stability of the experiments by ensuring that small volume variations during the experiments have negligible impacts.

C. Calibration

The proposed method involves a one-time calibration process to account for the effects of the setup, encompassing aspects such as microwave sensor design, liquid container dimensions, holder structure, manufacturing material, temperature, sensor location, and alignment between the sensor and

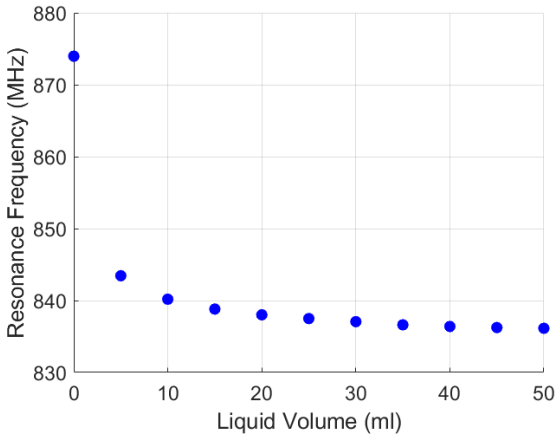

Fig. 10. First resonance frequency of the sensor versus the volume of ethanol in the container.

the liquid container. This calibration is only required to be performed once and does not need to be repeated as long as all the mentioned parameters remain the same. It is important to note that there is no need to recalibrate the sensing system when changing the LUT.

The calibration process consists of the first two steps in Fig. 5. It starts with extracting the dielectric spectra of the calibration liquids using the commercial dielectric probe shown in Fig. 6. The measured dielectric spectra for the calibration liquids are shown in Fig. 11.

Subsequently, the calibration liquids are introduced to the proposed system, and the resulting frequency shifts $\Delta f_{r,n}$ for all the resonance frequencies can be calculated as follows:

$$\Delta f_{r,n} = f_{r,n|\text{air}} - f_{r,n|\text{MUT}} \tag{6}$$

where $f_{r,n|\text{air}}$ and $f_{r,n|\text{MUT}}$ are the nth resonance frequencies of the sensor loaded with air and MUT, respectively. Table III shows the $\Delta f_{r,n}$ and the corresponding permittivity values $\epsilon'_{r|f_{r,n}}$ extracted from the calibration liquids. As expected, a larger $\Delta f_{r,n}$ corresponds to a higher $\epsilon'_{r|f_{r,n}}$ for a given harmonic.

Using the data in Table III, we can determine the calibration equations that describe the relationship between $\Delta f_{r,n}$ and $\epsilon'_{r|f_{r,n}}$ at the resonance frequencies. Since $\Delta f_{r,n} \propto 1/((\epsilon_{\text{eff}|f_{r,n}})_{MUT})^{1/2}$ as shown in (2) and $(\epsilon_{\text{eff}|f_{r,n}})_{MUT} \propto \epsilon'_{r|f_{r,n}}$, we have $\epsilon'_{r|f_{r,n}} \propto (1/\Delta f_{r,n})^2$. To model this relationship, we propose the following form for the calibration equations:

$$\hat{\epsilon}'_{r|f_{r,n}} = \left(\frac{k_1}{k_2 - \Delta f_{r,n}}\right)^2 + k_3 \tag{7}$$

where $\hat{\epsilon}'_{r|f_{r,n}}$ is the predicted real relative permittivity of the LUT at $f_{r,n}$ based on $\Delta f_{r,n}$ in MHz. k_1, k_2, and k_3 are the fitting parameters that can be extracted based on the experimental data shown in Table III. In this experiment, six calibration equations are determined for the six resonance frequencies. Fig. 12 shows the calibration curves fit to the experimental data, and the fitting parameters for the calibration curves are summarized in Table IV. These calibration curves allow us to predict the permittivity of an unknown LUT using the resonance frequency shifts.

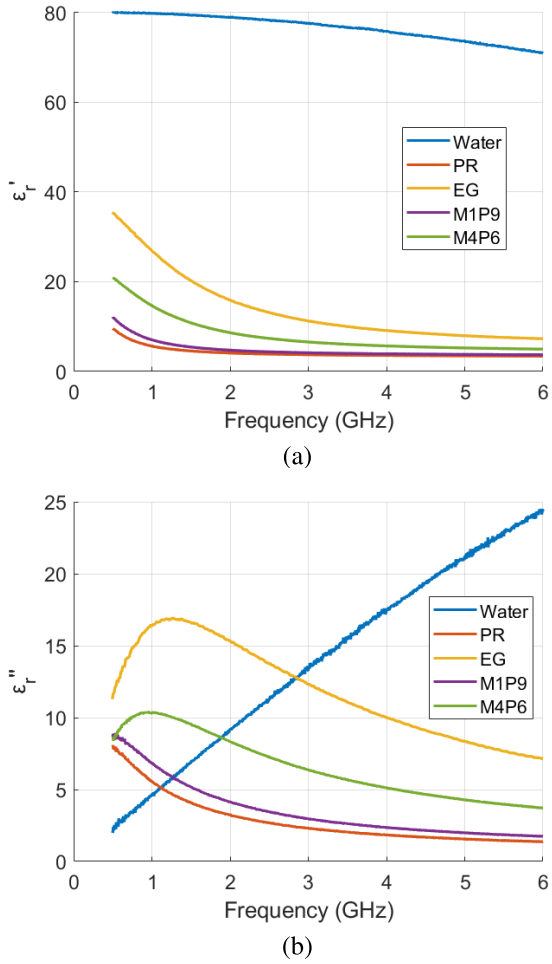

Fig. 11. (a) Real and (b) imaginary parts of the dielectric spectra of the calibration liquids measured by the commercial dielectric probe.

D. Dielectric Spectroscopy Extraction of the Unknown Liquids

Following the extraction of the calibration equations, it becomes possible to compute the entire dielectric spectrum of an unknown liquid, encompassing both the real and imaginary parts across the entire frequency range. The procedure starts by measuring all the resonance frequency shifts when introducing the test liquids to the microwave SRR shown in Fig. 7 (a). Using these frequency shifts, the permittivity of the LUT at the resonance frequencies can be calculated based on the calibration equations. Table V shows the predicted permittivity values for the test liquids at the resonance frequencies and compares them with the values obtained from the commercial dielectric probe. The predicted permittivity values closely match the dielectric probe values, with a root mean square error of 0.59.

Using the predicted permittivity values at the resonance frequencies, we can establish the Debye model for the LUT. The Debye model contains three unknown parameters: ϵ_s, ϵ_∞, and τ, which can be treated as the fitting parameters. These unknown parameters can be determined by fitting the real part of the Debye model in (4) to the predicted data. Subsequently, both the real and imaginary permittivity values at any desired frequency can be calculated using (4) and (5). This process

TABLE III
RESONANCE FREQUENCY SHIFTS AND THE CORRESPONDING PERMITTIVITY VALUES EXTRACTED FROM THE CALIBRATION LIQUIDS

Sample	Parameter	1^{st} Harmonic	2^{nd} Harmonic	3^{rd} Harmonic	4^{th} Harmonic	5^{th} Harmonic	6^{th} Harmonic
Water	$\Delta f_{r,n}$ (MHz)	58.67	48.35	47.33	110.44	175.47	161.55
	$\epsilon'_{r\|f_{r,n}}$	79.80	79.21	78.19	76.82	75.33	73.43
PR	$\Delta f_{r,n}$ (MHz)	26.76	19.62	14.82	31.32	53.33	58.49
	$\epsilon'_{r\|f_{r,n}}$	6.34	4.32	3.84	3.66	3.55	3.46
EG	$\Delta f_{r,n}$ (MHz)	48.35	39.35	30.66	72.35	120.28	120.76
	$\epsilon'_{r\|f_{r,n}}$	29.80	18.31	12.87	10.27	8.84	7.86
M1P9	$\Delta f_{r,n}$ (MHz)	30.48	22.32	16.98	35.33	59.57	64.55
	$\epsilon'_{r\|f_{r,n}}$	8.02	5.08	4.34	4.05	3.89	3.79
M4P6	$\Delta f_{r,n}$ (MHz)	40.07	31.38	24.24	52.49	85.49	89.15
	$\epsilon'_{r\|f_{r,n}}$	16.54	9.80	7.22	6.12	5.55	5.21

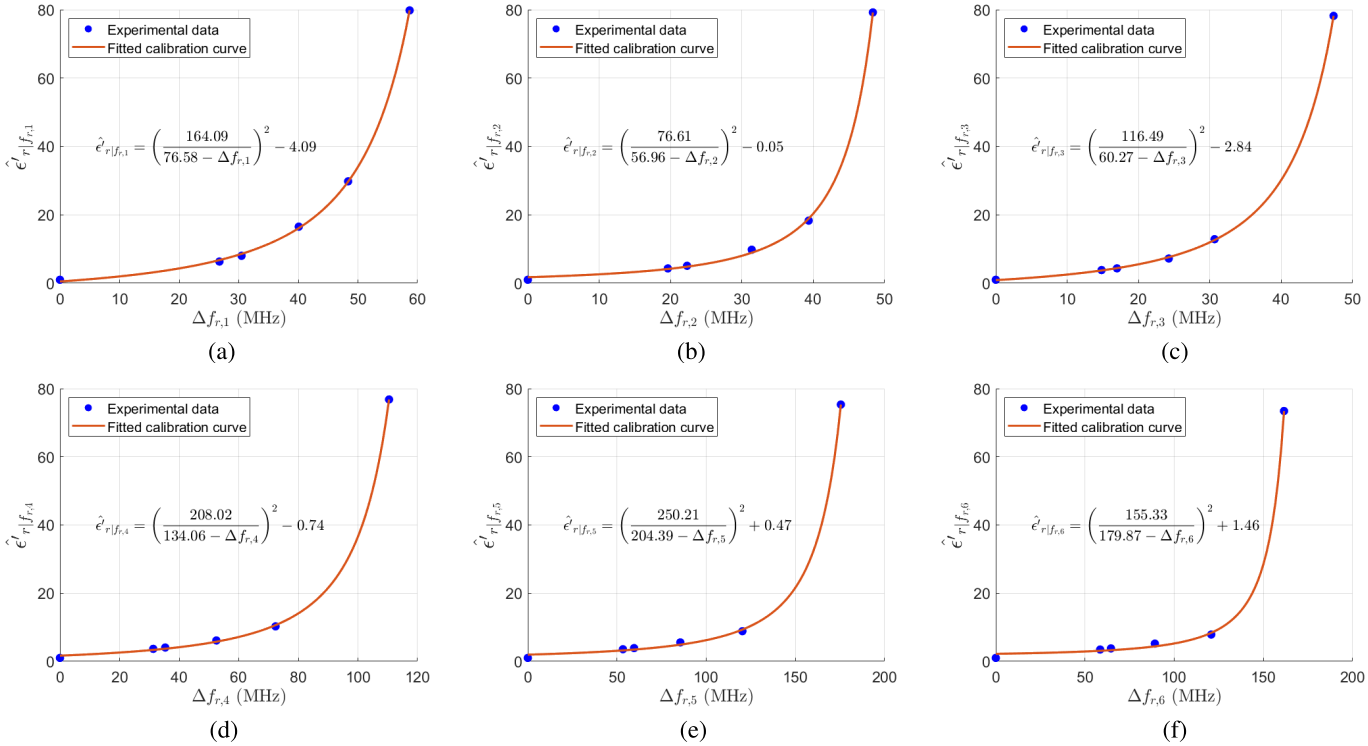

Fig. 12. Calibration curves and experimental data for (a) first resonance, (b) second resonance, (c) third resonance, (d) fourth resonance, (e) fifth resonance, and (f) sixth resonance.

TABLE IV
CALIBRATION EQUATION PARAMETERS FOR EACH RESONANCE

Resonance Number	k_1	k_2	k_3
1^{st} Resonance	164.09	76.58	-4.09
2^{nd} Resonance	76.61	56.96	-0.05
3^{rd} Resonance	116.49	60.27	-2.84
4^{th} Resonance	208.02	134.06	-0.74
5^{th} Resonance	250.21	204.39	0.47
6^{th} Resonance	155.33	179.87	1.46

allows us to extract the complete dielectric spectrum of the LUT. Figs. 13 and 14 present the real and imaginary dielectric spectra of the test liquids predicted using the proposed method, with a comparison to the values obtained from the commercial dielectric probe.

In Fig. 13, the predicted real permittivity closely aligns with the dielectric probe data within the frequency range of interest. In Fig. 14, the predicted imaginary permittivity spectrum matches the dielectric probe data at the upper frequency end in the frequency range of interest, and variations emerge at lower frequencies, particularly for certain liquids like M2E1P7 and M2P8, where the dielectric probe data diverges from the Debye model. This discrepancy can be caused by a major limitation of the commercial dielectric probe using the open probe method, which is a reduced accuracy at lower frequencies [12]. Consequently, the dielectric probe data, particularly for the imaginary part of the dielectric spectrum, is considered unreliable at lower frequencies. By disregarding data at lower frequencies and focusing on the higher frequency range, particularly above 1 GHz, the dielectric probe data for the imaginary part adheres to the Debye model, and the predicted spectrum aligns with the dielectric probe data. The Debye model parameters are summarized in Table VI.

To evaluate the performance of the proposed method, we can calculate the percentage error for each Debye model parameter using the following formula:

$$\%\text{error} = \left| \frac{x_{\text{predict}} - x_{\text{probe}}}{x_{\text{probe}}} \right| \times 100\% \tag{8}$$

TABLE V

PERMITTIVITY VALUES FOR THE TEST LIQUIDS AT THE RESONANCE FREQUENCIES (PREDICTION VERSUS PROBE)

Sample	Parameter	1^{st} Resonance	2^{nd} Resonance	3^{rd} Resonance	4^{th} Resonance	5^{th} Resonance	6^{th} Resonance
ET	Predicted ϵ_r'	15.34	8.05	6.83	5.34	4.64	4.13
	Probe ϵ_r'	16.51	9.52	6.95	5.87	5.32	4.99
M2E1P7	Predicted ϵ_r'	10.73	5.83	5.25	4.22	3.78	3.53
	Probe ϵ_r'	10.26	6.13	4.99	4.55	4.32	4.16
M2P8	Predicted ϵ_r'	11.07	5.94	5.30	4.23	3.81	3.54
	Probe ϵ_r'	10.65	6.32	5.09	4.60	4.38	4.21
M3E1P6	Predicted ϵ_r'	13.54	7.28	6.46	4.92	4.29	3.92
	Probe ϵ_r'	13.36	7.76	5.98	5.25	4.88	4.65
M3P7	Predicted ϵ_r'	13.59	7.25	6.38	4.89	4.28	3.90
	Probe ϵ_r'	13.48	7.86	6.02	5.27	4.89	4.66

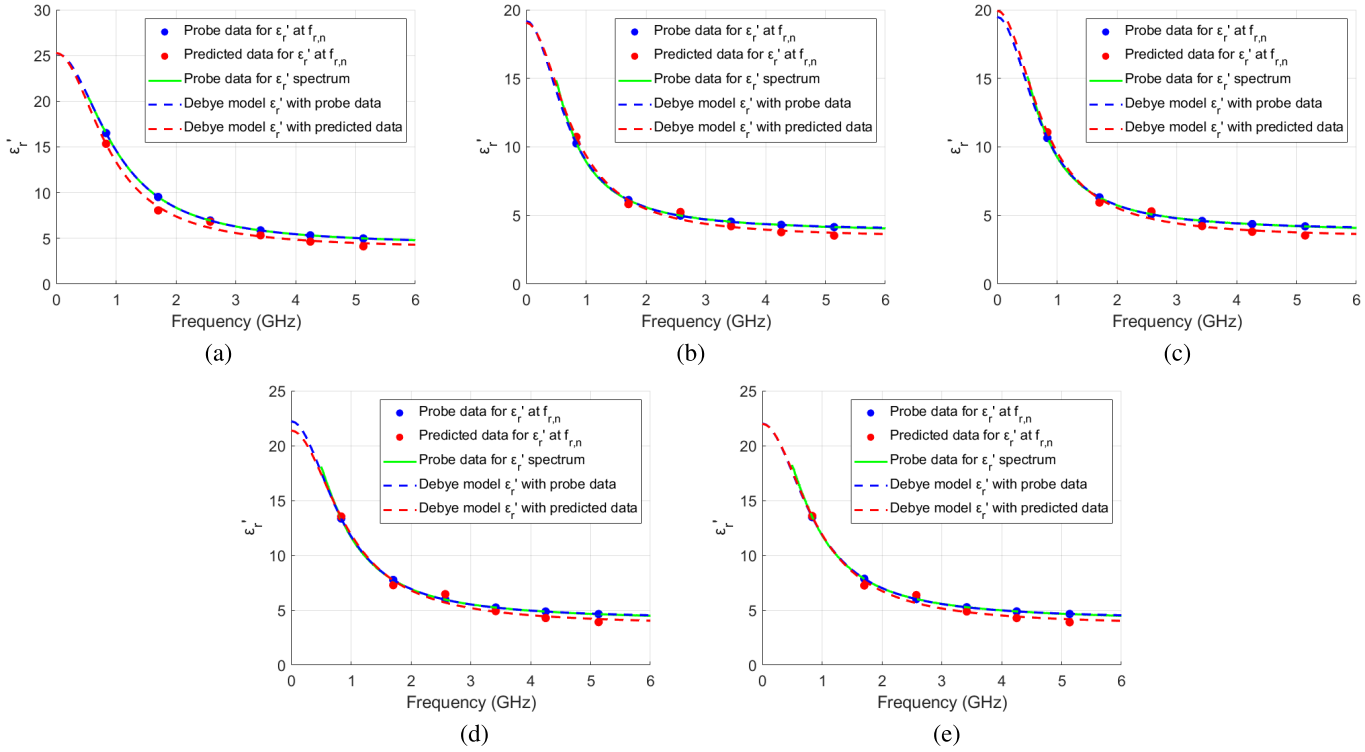

Fig. 13. Comparison of the predicted real permittivity spectrum using the proposed method with the data obtained from the commercial dielectric probe for the test liquids. (a) ET. (b) M2E1P7. (c) M2P8. (d) M3E1P6. (e) M3P7.

TABLE VI

DEBYE MODEL PARAMETERS FOR THE TEST LIQUIDS (PROPOSED METHOD VERSUS PROBE)

Sample	Parameter	ϵ_s	ϵ_∞	τ (ps)
ET	Proposed method	25.28	3.83	178.04
	Probe	25.24	4.25	161.12
M2E1P7	Proposed method	19.06	3.38	202.48
	Probe	19.18	3.90	224.72
M2P8	Proposed method	19.93	3.38	204.28
	Probe	19.48	3.92	217.49
M3E1P6	Proposed method	21.37	3.62	170.23
	Probe	22.22	4.19	187.32
M3P7	Proposed method	21.98	3.62	175.54
	Probe	22.01	4.17	182.30

where x_{predict} denotes the value obtained from our proposed method, and x_{probe} denotes the value obtained from the commercial dielectric probe in Fig. 6.

The ϵ_s parameter obtained from the proposed method closely matches those obtained from the commercial dielectric probe, with a negligible percentage error of 1.40%. This indicates that the proposed method is very accurate in determining the permittivity of the LUT at low frequencies. On the other hand, the percentage error for the ϵ_∞ parameter is 12.68%, which implies that the proposed method may exhibit relatively higher errors at very high frequencies. This is because the permittivity of the LUTs tends to be very low at high frequencies, making it more sensitive to variations and resulting in a higher percentage error. The percentage error for the τ parameter is 7.86%. Overall, the proposed method for dielectric spectroscopy demonstrates accurate performance, particularly when predicting values within the frequency band of interest.

One interesting aspect of the analysis involves exploring how errors in determining the Debye model parameters change with different numbers of resonance harmonics used in our proposed method for determining the permittivity spectrum of liquids. We conducted this analysis by applying the same

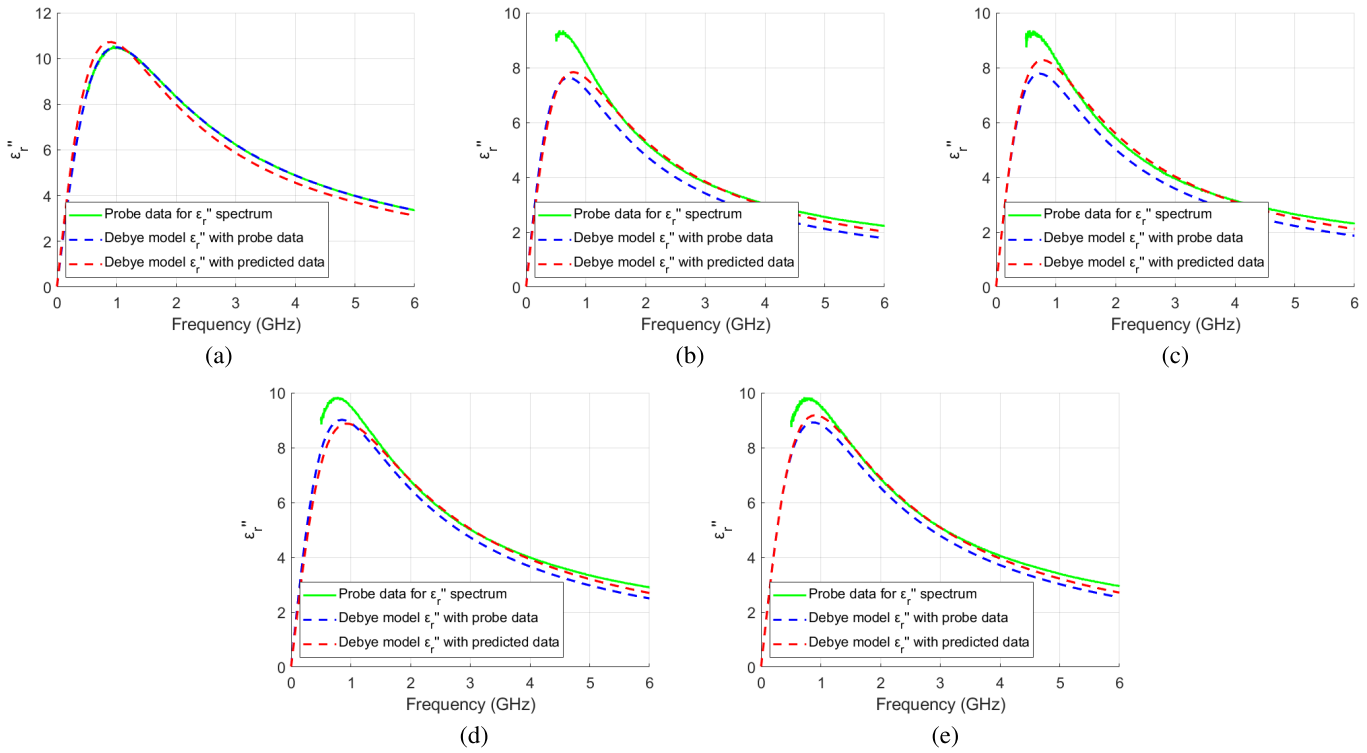

Fig. 14. Comparison of the predicted imaginary permittivity spectrum using the proposed method with the data obtained from the commercial dielectric probe for the test liquids. (a) ET. (b) M2E1P7. (c) M2P8. (d) M3E1P6. (e) M3P7.

procedures for determining the permittivity spectrum while using 4 to 6 harmonics of the ring resonator. Fig. 15 shows the average percentage error in the Debye model parameters in relation to the number of resonance harmonics, ranging from 4 to 6. The percentage error for ϵ_s decreases as we employ more resonance harmonics in our method. The percentage error for τ initially decreases when the number of resonance harmonics increases from 4 to 5 but then remains relatively constant after the increases from 5 to 6. The percentage error for ϵ_∞ gradually increases as the number of resonance harmonics increases from 4 to 6.

In this study, we utilized all six resonance harmonics within the frequency range of interest. This choice allows for better performance because the variation in ϵ_s has a more significant impact than the variation in ϵ_∞ on the predicted permittivity spectrum. To illustrate this, we conducted a sensitivity analysis using the Debye model of ethanol as an example, showcasing the permittivity spectrum's variation based on variations in the Debye model parameters. Fig. 16 shows the sensitivity analysis by considering the average percentage error arising from different numbers of resonance harmonics, ranging from 4 to 6. In each plot, two of the Debye model parameters were held constant, while the third parameter was varied with positive average percentage errors based on the different numbers of resonance harmonics. The sensitivity analysis indicates that the percentage error for ϵ_s has a more pronounced impact on performance than ϵ_∞ within the frequency range of interest. Therefore, although employing all six resonance harmonics results in a higher percentage error in ϵ_∞, the overall performance is better due to the lower percentage error for ϵ_s.

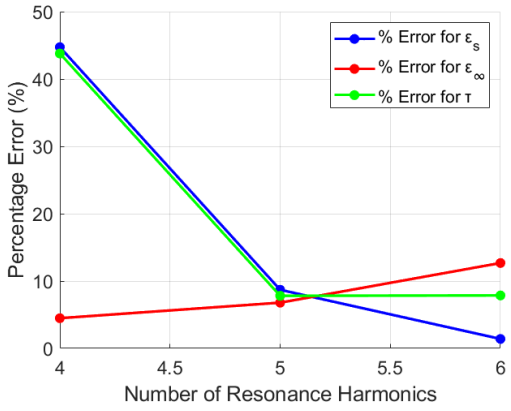

Fig. 15. Percentage error for Debye model parameters versus number of resonance harmonics.

Our proposed method for extracting the dielectric spectrum of liquids comes with certain limitations. One major constraint is the requirement to use the same setup for both calibration and testing. Any changes to the setup require recalibration to maintain prediction accuracy, emphasizing the importance of maintaining a standardized setup for reliable and consistent results. Another limitation is related to the assumption of neglected cross sensitivities of the resonance frequencies with the imaginary permittivity of the MUT. This assumption is based on the understanding that the resonance frequency shift of our SRR is determined mainly by the real part of the permittivity, with the effect of the imaginary part considered negligible in comparison as shown in Fig. 4. While we recognize that the resonance frequency shift of our SRR mainly depends on the real part of the permittivity, we also

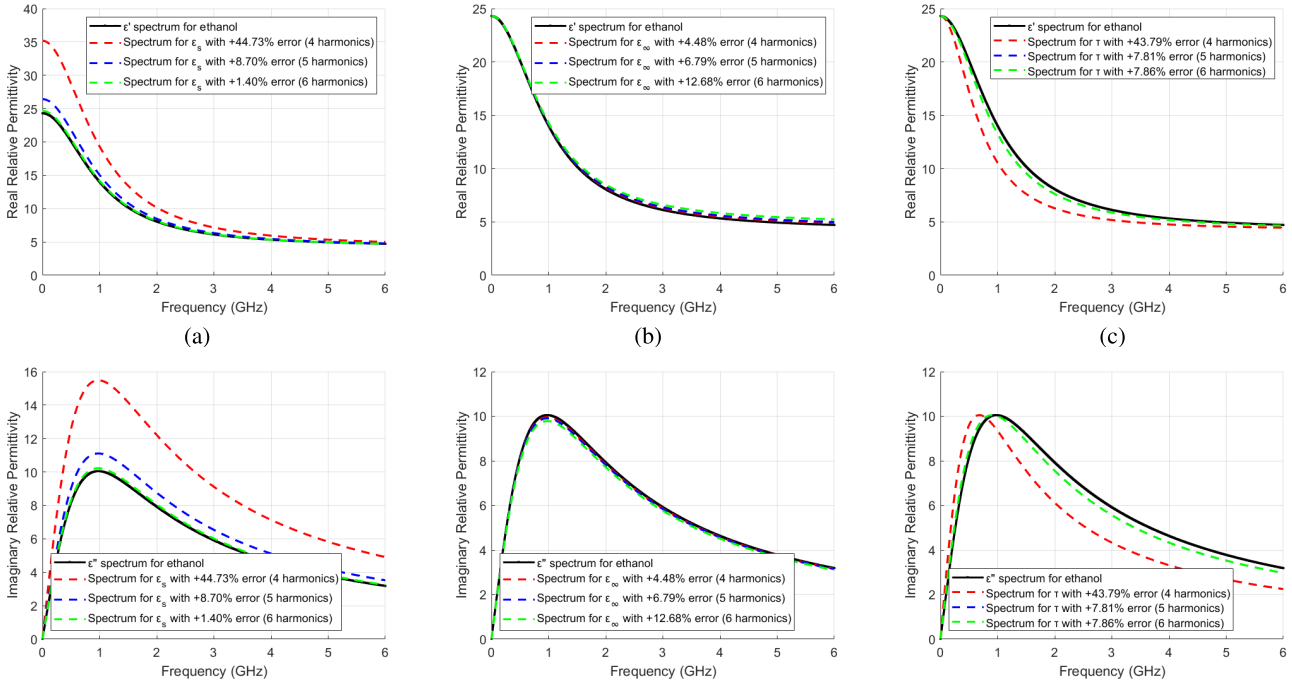

Fig. 16. Sensitivity analysis using ethanol as an example, with two Debye model parameters held constant while the third parameter is varied with positive average percentage error based on the number of resonance harmonics. (a) Real permittivity spectrum with varying ϵ_s. (b) Real permittivity spectrum with varying ϵ_∞. (c) Real permittivity spectrum with varying τ. (d) Imaginary permittivity spectrum with varying ϵ_s. (e) Imaginary permittivity spectrum with varying ϵ_∞. (f) Imaginary permittivity spectrum with varying τ. The results show that the percentage error for ϵ_s has a higher impact on performance than ϵ_∞ within the frequency range of interest.

acknowledge the minor impact on the frequency shift due to the cross sensitivity to the imaginary part of the permittivity, which might introduce some errors to the proposed system. Another limitation is associated with the assumption that the permittivity spectrum of the MUT adheres to the Debye model. While this assumption holds for many liquids, it may not be universally applicable. Liquids with complex dielectric behavior, such as specific ionic liquids and ferrofluids with intricate relaxation processes, might deviate from the Debye model [56], [57]. Future investigations could explore strategies to enhance the applicability of the proposed method, which may involve incorporating alternative permittivity models such as the Cole–Cole model, Havriliak–Negami model, or others, to accommodate a broader range of materials [50], [58].

One major drawback of the commercial dielectric probe with the open probe method is its low accuracy at lower frequencies, especially below 200 MHz and, in general, for materials which have low dielectric constants and loss factors [12]. On the other hand, our proposed method enables the calculation of permittivity using the Debye model at any frequency, including lower frequencies and frequencies beyond our originally targeted band. The proposed method offers a cost-effective alternative to commercial dielectric probe devices. Furthermore, it can complement other dielectric probe methods such as the open probe method to enhance overall accuracy in the permittivity measurement.

IV. Conclusion

An innovative method is presented for wideband dielectric spectroscopy using a simple microwave SRR. The proposed method utilizes the multiresonance property of the SRR to extract the entire dielectric spectrum of a liquid with the Debye model. For demonstration, an experiment with five calibration samples and five test samples is conducted, and the extracted data from the proposed method is compared with those obtained from a commercial dielectric probe. Following a one-time calibration process, the proposed method demonstrated high precision in predicting real permittivity values at the resonance frequencies, achieving a low root mean square error of 0.59. By fitting these data points to a Debye model, the entire dielectric spectrum of the LUT can be calculated. The proposed method achieved high accuracy with a percentage error of 1.40% for the ϵ_s parameter and 7.86% for the τ parameter. While the performance of the proposed method showed a slight decrease at higher frequencies, with a 12.68% error in the ϵ_∞ parameter, it is noteworthy that within the target frequency range, the data from the proposed method closely aligns with the data obtained from the commercial dielectric probe.

The proposed method for wideband dielectric spectroscopy using a microwave SRR achieves accurate results while being low-cost, simple to use, and easy to fabricate. Its potential application extends across various fields including oil and gas industries, chemical analysis, and biosensing.

Acknowledgment

The authors would like to thank Dr. Rashid Mirzavand and Dr. Ramin Khosravi for generously providing access to their laboratory facilities.

REFERENCES

[1] T. P. Iglesias and S. M. Pereira, "Distributed parameters for low-frequency dielectric characterization of liquids with open-ended coaxial cell," *IEEE Trans. Instrum. Meas.*, vol. 55, no. 1, pp. 176–179, Feb. 2006, doi: 10.1109/TIM.2005.861499.

[2] H. Suzuki and T. Kamijo, "Millimeter-wave measurement of complex permittivity by perturbation method using open resonator," *IEEE Trans. Instrum. Meas.*, vol. 57, no. 12, pp. 2868–2873, Dec. 2008.

[3] H. Chen, H. Chen, W. Che, S. Zheng, X. Xiu, and Q. Xue, "Review and modification of permittivity measurement on open resonator for transparent material measurements at terahertz," *IEEE Trans. Instrum. Meas.*, vol. 69, no. 11, pp. 9144–9156, Nov. 2020.

[4] K. Folgero, "Broad-band dielectric spectroscopy of low-permittivity fluids using one measurement cell," *IEEE Trans. Instrum. Meas.*, vol. 47, no. 4, pp. 881–885, Aug. 1998, doi: 10.1109/19.744637.

[5] J. Sun and S. Lucyszyn, "Extracting complex dielectric properties from reflection-transmission mode spectroscopy," *IEEE Access*, vol. 6, pp. 8302–8321, 2018.

[6] J. Baker-Jarvis, E. J. Vanzura, and W. A. Kissick, "Improved technique for determining complex permittivity with the transmission/reflection method," *IEEE Trans. Microwave Theory Techn.*, vol. 38, no. 8, pp. 1096–1103, Aug. 1990.

[7] Z. Ma and S. Okamura, "Permittivity determination using amplitudes of transmission and reflection coefficients at microwave frequency," *IEEE Trans. Microwave Theory Techn.*, vol. 47, no. 5, pp. 546–550, May 1999.

[8] S. A. Komarov, A. S. Komarov, D. G. Barber, M. J. L. Lemes, and S. Rysgaard, "Open-ended coaxial probe technique for dielectric spectroscopy of artificially grown sea ice," *IEEE Trans. Geosci. Remote Sens.*, vol. 54, no. 8, pp. 4941–4951, Aug. 2016.

[9] D. Popovic and M. Okoniewski, "Effects of mechanical flaws in open-ended coaxial probes for dielectric spectroscopy," *IEEE Microwave Wireless Compon. Lett.*, vol. 12, no. 10, pp. 401–403, Oct. 2002, doi: 10.1109/LMWC.2002.803192.

[10] D. Popovic et al., "Precision open-ended coaxial probes for in vivo and ex vivo dielectric spectroscopy of biological tissues at microwave frequencies," *IEEE Trans. Microwave Theory Techn.*, vol. 53, no. 5, pp. 1713–1722, May 2005.

[11] B. L. McLaughlin and P. A. Robertson, "Submillimeter coaxial probes for dielectric spectroscopy of liquids and biological materials," *IEEE Trans. Microwave Theory Techn.*, vol. 57, no. 12, pp. 3000–3010, Dec. 2009, doi: 10.1109/TMTT.2009.2034222.

[12] V. Matko and M. Milanovič, "Sensitivity and accuracy of dielectric measurements of liquids significantly improved by coupled capacitive-dependent quartz crystals," *Sensors*, vol. 21, no. 10, p. 3565, May 2021.

[13] S. Chen, K. A. Korolev, J. Kupershmidt, K. Nguyen, and M. N. Afsar, "High-resolution high-power quasi-optical free-space spectrometer for dielectric and magnetic measurements in millimeter waves," *IEEE Trans. Instrum. Meas.*, vol. 58, no. 8, pp. 2671–2678, Aug. 2009, doi: 10.1109/TIM.2009.2015699.

[14] T. Tosaka, K. Fujii, K. Fukunaga, and A. Kasamatsu, "Development of complex relative permittivity measurement system based on free-space in 220–330-GHz range," *IEEE Trans. Terahertz Sci. Technol.*, vol. 5, no. 1, pp. 102–109, Jan. 2015, doi: 10.1109/TTHZ.2014.2362013.

[15] R. Ebrahimi Ghiri, A. Pourghorban Saghati, E. Kaya, and K. Entesari, "A miniaturized contactless UWB microwave system for time-domain dielectric spectroscopy," *IEEE Trans. Microwave Theory Techn.*, vol. 65, no. 12, pp. 5334–5344, Dec. 2017, doi: 10.1109/TMTT.2017.2768032.

[16] Z. Chen, Y. Shao, and P. Wang, "Resonator- and filter-induced slow waves for high-sensitivity RF interferometer operations," *IEEE Sensors J.*, vol. 15, no. 5, pp. 2993–2999, May 2015, doi: 10.1109/JSEN.2014.2386254.

[17] V. V. Parshin, M. Y. Tretyakov, M. A. Koshelev, and E. A. Serov, "Modern resonator spectroscopy at submillimeter wavelengths," *IEEE Sensors J.*, vol. 13, no. 1, pp. 18–23, Jan. 2013, doi: 10.1109/JSEN.2012.2215315.

[18] M. G. Mayani, F. J. Herraiz-Martínez, J. M. Domingo, R. Giannetti, and C. R. García, "Dual-band metamaterial-inspired microwave sensor for liquid dielectric spectroscopy," in *Proc. IEEE Int. Instrum. Meas. Technol. Conf.*, Glasgow, United Kingdom, May 2021, pp. 1–5, doi: 10.1109/I2MTC50364.2021.9460055.

[19] A. Ebrahimi, J. Scott, and K. Ghorbani, "Ultrahigh-sensitivity microwave sensor for microfluidic complex permittivity measurement," *IEEE Trans. Microwave Theory Techn.*, vol. 67, no. 10, pp. 4269–4277, Oct. 2019.

[20] T. Chretiennot, D. Dubuc, and K. Grenier, "A microwave and microfluidic planar resonator for efficient and accurate complex permittivity characterization of aqueous solutions," *IEEE Trans. Microwave Theory Techn.*, vol. 61, no. 2, pp. 972–978, Feb. 2013, doi: 10.1109/TMTT.2012.2231877.

[21] Y. Chen, J. Huang, Y. Xiang, L. Fu, W. Gu, and Y. Wu, "A modified SIW re-entrant microfluidic microwave sensor for characterizing complex permittivity of liquids," *IEEE Sensors J.*, vol. 21, no. 13, pp. 14838–14846, Jul. 2021.

[22] M. Abdolrazzaghi, M. Daneshmand, and A. K. Iyer, "Strongly enhanced sensitivity in planar microwave sensors based on metamaterial coupling," *IEEE Trans. Microwave Theory Techn.*, vol. 66, no. 4, pp. 1843–1855, Apr. 2018.

[23] G. Govind and M. J. Akhtar, "Metamaterial-inspired microwave microfluidic sensor for glucose monitoring in aqueous solutions," *IEEE Sensors J.*, vol. 19, no. 24, pp. 11900–11907, Dec. 2019.

[24] P. Loutchanwoot and S. Harnsoongnoen, "Microwave microfluidic sensor for detection of high equol concentrations in aqueous solution," *IEEE Trans. Biomed. Circuits Syst.*, vol. 16, no. 2, pp. 244–251, Apr. 2022.

[25] M. H. Zarifi, H. Sadabadi, S. H. Hejazi, M. Daneshmand, and A. Sanati-Nezhad, "Noncontact and nonintrusive microwave-microfluidic flow sensor for energy and biomedical engineering," *Sci. Rep.*, vol. 8, no. 1, Jan. 2018, Art. no. 1, doi: 10.1038/S41598-017-18621-2.

[26] Z. Abbasi, M. Baghelani, M. Nosrati, A. Sanati-Nezhad, and M. Daneshmand, "Real-time non-contact integrated chipless RF sensor for disposable microfluidic applications," *IEEE J. Electromagn., RF Microwave Med. Biol.*, vol. 4, no. 3, pp. 171–178, Sep. 2020.

[27] M. Nosrati, Z. Abbasi, M. Baghelani, S. Bhadra, and M. Daneshmand, "Locally strong-coupled microwave resonator using PEMC boundary for distant sensing applications," *IEEE Trans. Microwave Theory Techn.*, vol. 67, no. 10, pp. 4130–4139, Oct. 2019.

[28] M. Abdolrazzaghi, N. Katchinskiy, A. Y. Elezzabi, P. E. Light, and M. Daneshmand, "Noninvasive glucose sensing in aqueous solutions using an active split-ring resonator," *IEEE Sensors J.*, vol. 21, no. 17, pp. 18742–18755, Sep. 2021.

[29] L. V. Herrera-Sepulveda, J. L. Olvera-Cervantes, A. Corona-Chavez, and T. Kaur, "Sensor and methodology for determining dielectric constant using electrically coupled resonators," *IEEE Microwave Wireless Compon. Lett.*, vol. 29, no. 9, pp. 626–628, Sep. 2019.

[30] C. G. Juan et al., "Study Qu-based resonant microwave sensors and design of 3-D-Printed devices dedicated to glucose monitoring," *IEEE Trans. Instrum. Meas.*, vol. 70, pp. 1–16, 2021, doi: 10.1109/TIM.2021.3122525.

[31] P. Vélez et al., "Single-frequency amplitude-modulation sensor for dielectric characterization of solids and microfluidics," *IEEE Sensors J.*, vol. 21, no. 10, pp. 12189–12201, May 2021.

[32] J. Mu noz-Enano, P. Vélez, L. Su, M. Gil, P. Casacuberta, and F. Martín, "On the sensitivity of reflective-mode phase-variation sensors based on open-ended stepped-impedance transmission lines: Theoretical analysis and experimental validation," *IEEE Trans. Microwave Theory Techn.*, vol. 69, no. 1, pp. 308–324, Jan. 2021.

[33] P. Casacuberta, P. Vélez, J. Mu noz-Enano, L. Su, and F. Martín, "Highly sensitive reflective-mode phase-variation permittivity sensors using coupled line sections," *IEEE Trans. Microwave Theory Techn.*, vol. 71, no. 7, pp. 2970–2984, Jul. 2023.

[34] C. G. Juan, E. Bronchalo, B. Potelon, C. Quendo, E. Ávila-Navarro, and J. M. Sabater-Navarro, "Concentration measurement of microliter-volume water-glucose solutions using Q factor of microwave sensors," *IEEE Trans. Instrum. Meas.*, vol. 68, no. 7, pp. 2621–2634, Jul. 2019, doi: 10.1109/TIM.2018.2866743.

[35] A. Ebrahimi et al., "Highly sensitive phase-variation dielectric constant sensor based on a capacitively-loaded slow-wave transmission line," *IEEE Trans. Circuits Syst. I, Reg. Papers*, vol. 68, no. 7, pp. 2787–2799, Jul. 2021.

[36] P. Vélez, L. Su, K. Grenier, J. Mata-Contreras, D. Dubuc, and F. Martín, "Microwave microfluidic sensor based on a microstrip splitter/combiner configuration and split ring resonators (SRRs) for dielectric characterization of liquids," *IEEE Sensors J.*, vol. 17, no. 20, pp. 6589–6598, Oct. 2017.

[37] M. C. Jain, A. V. Nadaraja, B. M. Vizcaino, D. J. Roberts, and M. H. Zarifi, "Differential microwave resonator sensor reveals glucose-dependent growth profile of E. Coli on solid agar," *IEEE Microwave Wireless Compon. Lett.*, vol. 30, no. 5, pp. 531–534, May 2020, doi: 10.1109/LMWC.2020.2980756.

[38] S. Mohammadi and M. H. Zarifi, "Differential microwave resonator sensor for real-time monitoring of volatile organic compounds," *IEEE Sensors J.*, vol. 21, no. 5, pp. 6105–6114, Mar. 2021.

[39] A. Ebrahimi and K. Ghorbani, "High-sensitivity detection of solid and liquid dielectrics using a branch line coupler sensor," *IEEE Trans. Microwave Theory Techn.*, vol. 71, no. 12, pp. 5233–5245, Dec. 2023.

[40] A. Ebrahimi, J. Scott, and K. Ghorbani, "Differential sensors using microstrip lines loaded with two split-ring resonators," *IEEE Sensors J.*, vol. 18, no. 14, pp. 5786–5793, Jul. 2018.

[41] Z. Abbasi, M. Baghelani, and M. Daneshmand, "High-resolution chipless tag RF sensor," *IEEE Trans. Microwave Theory Techn.*, vol. 68, no. 11, pp. 4855–4864, Nov. 2020, doi: 10.1109/TMTT.2020.3014653.

[42] H. Lobato-Morales, A. Corona-Chavez, J. L. Olvera-Cervantes, R. A. Chavez-Perez, and J. L. Medina-Monroy, "Wireless sensing of complex dielectric permittivity of liquids based on the RFID," *IEEE Trans. Microwave Theory Techn.*, vol. 62, no. 9, pp. 2160–2167, Sep. 2014.

[43] M. Baghelani, Z. Abbasi, M. Daneshmand, and P. E. Light, "Non-invasive continuous-time glucose monitoring system using a chipless printable sensor based on split ring microwave resonators," *Sci. Rep.*, vol. 10, no. 1, Jul. 2020, Art. no. 1, doi: 10.1038/S41598-020-69547-1.

[44] N. Kazemi, M. Abdolrazzaghi, and P. Musilek, "Comparative analysis of machine learning techniques for temperature compensation in microwave sensors," *IEEE Trans. Microwave Theory Techn.*, vol. 69, no. 9, pp. 4223–4236, Sep. 2021.

[45] N. Kazemi, M. Abdolrazzaghi, P. Musilek, and M. Daneshmand, "A temperature-compensated high-resolution microwave sensor using artificial neural network," *IEEE Microwave Wireless Compon. Lett.*, vol. 30, no. 9, pp. 919–922, Sep. 2020.

[46] N. Hosseini, M. Baghelani, and M. Daneshmand, "Selective volume fraction sensing using resonant-based microwave sensor and its harmonics," *IEEE Trans. Microwave Theory Techn.*, vol. 68, no. 9, pp. 3958–3968, Sep. 2020.

[47] P. A. Bernard and J. M. Gautray, "Measurement of dielectric constant using a microstrip ring resonator," *IEEE Trans. Microwave Theory Techn.*, vol. 39, no. 3, pp. 592–595, Mar. 1991.

[48] C.-S. Lee and C.-L. Yang, "Complementary split-ring resonators for measuring dielectric constants and loss tangents," *IEEE Microwave Wireless Compon. Lett.*, vol. 24, no. 8, pp. 563–565, Aug. 2014.

[49] X. Han et al., "Microwave sensor loaded with complementary curved ring resonator for material permittivity detection," *IEEE Sensors J.*, vol. 22, no. 21, pp. 20456–20463, Nov. 2022.

[50] K. S. Cole and R. H. Cole, "Dispersion and absorption in dielectrics I. Alternating current characteristics," *J. Chem. Phys.*, vol. 9, no. 4, pp. 341–351, Apr. 1941.

[51] S. Holm, "Time domain characterization of the cole-cole dielectric model," *J. Electr. Bioimpedance*, vol. 11, no. 1, pp. 101–105, Dec. 2020, doi: 10.2478/JOEB-2020-0015.

[52] F. Buckley and A. A. Maryott. (1958). *Circular Bureau Standards 589: Tables Dielectric Dispersion Data for Pure Liquids Dilute Solutions.* Accessed: Sep. 13, 2023. [Online]. Available: http://archive.org/details/circularofbureau589buck

[53] D. M. Pozar, *Microwave Engineering*, 4th ed. Hoboken, NJ, USA: Wiley, 2012.

[54] M. S. Boybay and O. M. Ramahi, "Material characterization using complementary split-ring resonators," *IEEE Trans. Instrum. Meas.*, vol. 61, no. 11, pp. 3039–3046, Nov. 2012.

[55] M. S. Boybay and O. M. Ramahi, "Non-destructive thickness measurement using quasi-static resonators," *IEEE Microwave Wireless Compon. Lett.*, vol. 23, no. 4, pp. 217–219, Apr. 2013, doi: 10.1109/LMWC.2013.2249056.

[56] Y. Wang, "Low-frequency dynamics in ionic liquids: Comparison of experiments and the random barrier model," *Phys. Chem. Chem. Phys.*, vol. 24, no. 27, pp. 16501–16511, 2022, doi: 10.1039/D2CP01858F.

[57] A. Joseph, J. Fal, A. Bak, S. Mathew, and G. Żyła, "Complex dielectric response and EDL characteristics of different types of ionic liquid iron oxide nanofluids (ionanofluids)," *Chem. Phys. Impact*, vol. 7, Dec. 2023, Art. no. 100357, doi: 10.1016/J.CHPHI.2023.100357.

[58] S. Havriliak and S. Negami, "A complex plane representation of dielectric and mechanical relaxation processes in some polymers," *Polymer*, vol. 8, pp. 161–210, Jan. 1967.

Wendi Zhu (Graduate Student Member, IEEE) received the B.Eng. degree in electrical engineering from Carleton University, Ottawa, ON, Canada, in 2022. He is currently pursuing the M.Sc. degree in electrical and computer engineering at University of Alberta, Edmonton, AB, Canada.

His research interests include microwave sensors, biosensors, antennas, and RF/microwave circuit design.

Masoud Baghelani (Senior Member, IEEE) received the B.S. degree in electrical engineering from Chamran University, Ahvaz, Iran, in 2005, and the M.Sc. and Ph.D. degrees in electrical engineering from the Sahand University of Technology, Tabriz, Iran, in 2009 and 2013, respectively.

From 2013 to 2018, he was an Assistant Professor with the Electrical Engineering Department, Ilam University, Ilam, Iran, where he was promoted as an Associate Professor in 2018. From 2018 to 2020, he was a Postdoctoral Fellow with the Microwave to mmWave Laboratory, University of Alberta, Edmonton, AB, Canada, where he is currently an Adjunct Professor with the Department of Electrical and Computer Engineering. He is also the Director of the Microsystems and Advanced Instrumentation Laboratory, University of Ilam. His research interests include microwave sensors for industrial and biomedical applications, radio frequency microelectromechanical system (RF MEMS) resonators and switches for communication applications, and RF microelectronics.

Dr. Baghelani was a recipient of the Best Industrial Academic Research Project Award in Iran, in 2018. He also received the Best Entrepreneur Award in Ilam Province, Iran, in 2016 and 2017 for his works on Kavosh Electronics Soushian "Knowledge-Based" company certified by the Iranian Vice-President for Science and Technology. He is currently the CTO of FringeField Technologies Inc.—an Alberta-based start-up active in the area of noninvasive biomarker monitoring.

Ashwin K. Iyer (Senior Member, IEEE) received the B.A.Sc. (Hons.), M.A.Sc., and Ph.D. degrees in electrical engineering from the University of Toronto, Toronto, ON, Canada, in 2001, 2003, and 2009, respectively, where he was involved in the discovery and development of the negative refractive index transmission line approach to metamaterial design and the realization of metamaterial lenses for free-space microwave subdiffraction imaging.

He is currently a Professor with the Department of Electrical and Computer Engineering, University of Alberta, Edmonton, AB, Canada, where he serves as the Director of the Microwave, Millimetre-Wave, and MetaDevices (M3) Laboratory. His research interests include novel RF/microwave circuits and techniques, fundamental electromagnetic theory, antennas, sensors, and engineered metamaterials, with an emphasis on their applications to microwave and optical devices, defense technologies, and biomedicine. He has coauthored a number of highly cited papers and four book chapters on the subject of metamaterials.

Dr. Iyer is a member of several IEEE AP-S committees including its Administrative Committee. He was a recipient of the IEEE AP-S R. W. P. King Award in 2008, the IEEE AP-S Donald G. Dudley Jr. Undergraduate Teaching Award in 2015, the University of Alberta Provost's Award for Early Achievement of Excellence in Undergraduate Teaching in 2014, and the University of Alberta Rutherford Award for Excellence in Undergraduate Teaching in 2018. His students are the recipients of several major national and international awards for their research. He served as a Technical Program Committee Co-Chair for the 2020, 2016, and 2015 AP-S/URSI International Symposia. He serves as the Chair for the IEEE Northern Canada Section's Award-Winning Joint Chapter of the AP-S and MTT-S. From 2012 to 2018, he was an Associate Editor of IEEE TRANSACTIONS ON ANTENNAS AND PROPAGATION. He currently serves as a Track Editor. He was also a Guest Editor for IEEE TRANSACTIONS ON ANTENNAS AND PROPAGATION Special Issue on Recent Advances in Metamaterials and Metasurfaces. He is a Registered Member of the Association of Professional Engineers and Geoscientists of Alberta.